PHYSICAL REVIEW B **77**, 020101(R) (2008)

# Theoretical study of the structure of calcium in phases IV and V via *ab initio* metadynamics simulation

Takahiro Ishikawa,* Ayako Ichikawa, Hitose Nagara, Masaaki Geshi, Koichi Kusakabe, and Naoshi Suzuki
*Division of Frontier Materials Science, Graduate School of Engineering Science, Osaka University, Toyonaka, Osaka 560-8531, Japan*
(Received 5 September 2007; revised manuscript received 9 November 2007; published 17 January 2008)

We searched for the structure of calcium in phases IV and V by a metadynamics simulation based on *ab initio* calculations, and found two structures. One is a tetragonal lattice which consists of two helical chains along the *c* axis. The other is an orthorhombic lattice of four zigzag chains. We have calculated the x-ray diffraction patterns and enthalpies of the two structures discovered by our simulation. From comparisons of the patterns with the experimental x-ray patterns of the phases IV and V and from the pressure dependence of the enthalpies, we conclude that the structure with a helical pattern corresponds to phase IV and the structure with a zigzag pattern to phase V.

DOI: 10.1103/PhysRevB.77.020101 PACS number(s): 61.50.Ah, 61.50.Ks, 62.50.−p, 64.70.K−

Studies have revealed that many elements have complex structures with low symmetry at high pressures; McMahon and Nelmes have reviewed complex lattice structures of elements under high pressure.[1] Some elements have interesting structures beyond the simple cubic (sc) lattice at high pressure. Phosphorus has the sc structure (P-III) from 10 to 107 GPa,[2] which transforms, at 107 GPa, to a complex structure[3] (P-IV) whose structure has long been unidentified. But it has recently been theoretically predicted[4] and experimentally confirmed[5] to be an incommensurately modulated structure.

Another example is calcium, which shows interesting successive structural phase transitions under pressure, where the transitions are from a closest-packed to a less close-packed structure. The fcc structure at ambient pressure transforms to the bcc at 20 GPa and then to the sc structure (Ca-III) at 32 GPa.[6] In 2005 Yabuuchi *et al.* pressurized calcium further and observed new structural phase transitions.[7] The sc transforms to phase IV (Ca-IV) at 113 GPa and then to phase V (Ca-V) at 139 GPa.[7] Very recently an increase of the superconducting transition temperature $T_c$ in the high-pressure phases has also been reported, i.e., 25 K at 161 GPa in Ca-V, which is the highest recorded for an element.[8] This result has attracted much interest in relation to pressure-induced electronic *s-d* transfer and the increase of the superconducting $T_c$ with pressure, which has been discussed also in Sr and Ba under pressure.[9–11] Information about the structures of Ca-IV and Ca-V is crucial for the clarification of the high $T_c$ in calcium.

In this work, we have explored the crystal structures of Ca-IV and Ca-V using an *ab initio* metadynamics simulation[12] in which we employed density functional theory in the generalized gradient approximation (GGA). Metadynamics is a method used to find neighboring local minima by filling the potential wells with an artificial Gaussian potential (GP). To avoid rigid rotation of the system, we treated only the symmetric part of the cell matrix defined by $\mathbf{h}=(\vec{a},\vec{b},\vec{c})$, where $\vec{a}$, $\vec{b}$, and $\vec{c}$ are the lattice vectors. We update the simulation cell by the steepest-descent method with a stepping parameter $\delta h$: $\mathbf{h}_{ij}^{t+1}=\mathbf{h}_{ij}^{t}+\delta h\mathbf{F}_{ij}^{t}/|\mathbf{F}_{ij}^{t}|$, where $t$ is the number of updates of $\mathbf{h}$ and $\mathbf{F}$ is the driving force for the update. If we denote the Gibbs potential by $G_o(\mathbf{h}^t)$ and define the GP by $G_g(\mathbf{h}^t)=\Sigma_{t'<t}\Pi_{i,j}W\exp(-[\mathbf{h}^t-\mathbf{h}^{t'}]_{ij}^2/2\delta h^2)$, the driving force $\mathbf{F}_{ij}^t$ is the sum of $\mathbf{F}_{oij}^t=-\partial G_o(\mathbf{h}^t)/\partial\mathbf{h}_{ij}$ and $\mathbf{F}_{gij}^t=-\partial G_g(\mathbf{h}^t)/\partial\mathbf{h}_{ij}$. We define one update of $\mathbf{h}$ as one metastep, and between the metasteps we run about 100 steps of a conventional molecular dynamics (MD) simulation for the equilibration of the system with a fixed cell to obtain good estimates of the internal stress to define $\mathbf{F}_o^t$. We used the PWSCF code[13] for the fixed-cell MD in this simulation.

For the exchange-correlation energy functional in the GGA, we employed the expression by Perdew and Wang[14] and used an ultrasoft pseudopotential. To examine the parameters of the pseudopotential, we checked localization of semicore orbitals on the calcium atom using the full-potential augmented plane-wave plus local orbitals method, which is embodied in the WIEN2K code.[15] The $2p$ level lies at about 331 eV below the Fermi energy and it is deep enough in energy for a core state, but the $3s$ level lies only about 43.3 eV below the Fermi energy and the corresponding charge is not completely confined inside the touching atomic sphere. Thus, for the pseudopotential, we regarded ten electrons in the $3s$, $3p$, and $4s$ states as the valence electrons.

In the simulation, we first run the metadynamics simulation steps with $W=0$, which we call a preparative run, to find a local minimum on the Gibbs free energy (GFE) surface near the initial structure. The structure obtained by the preparative run is used as the starting structure of the succeeding metadynamics simulation. Starting the metadynamics simulation with a GP, which we call the main run, we explore other local minima. After observing the changes in the character of the evolution of the unit cell parameters, we switch the GP off again and relax the system by a metadynamics simulation similar to the preparative run, which we call the relaxation run. For the structures obtained, we calculate x-ray diffraction patterns. The enthalpies are also calculated and compared among the local minima. This procedure is repeated to find the most probable structure.

We have chosen, as the initial simulation cell, a cubic supercell whose edge length is 4.50 Å. In the simulation cell we put eight Ca atoms at (0,0,0), (0.5,0,0), (0,0.5,0), (0.5,0.5,0), (0,0,0.5), (0.5,0,0.5), (0,0.5,0.5), and (0.5,0.5,0.5) in fractional coordinates to make the sc structure. We performed the **k**-space integration using $8\times8\times8$ mesh points

 

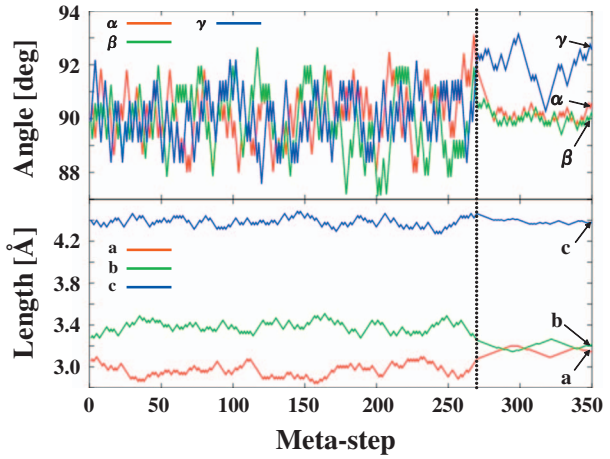


FIG. 1. (Color) Evolution of the cell parameters in the *ab initio* metadynamics simulation. First the Gaussian potential parameters $W$ and $\delta h$ were set at 10 mRy and 20 mÅ, respectively, and then the Gaussian potential was switched off after the 270th metastep by setting $W$ at 0 mRy.

in the first Brillouin zone and set the energy cutoff of the plane-wave basis at 24 Ry. For the optimized structure obtained by the simulation, we checked the accuracy of the calculation by changing the energy cutoff from 24 to 40 Ry. Along the lines of the simulation stated above, we started the preparative run at 120 GPa by setting the value of $W$ at 0 mRy and $\delta h$ to 10 mÅ and explored the starting local minimum. In this run, the cubic supercell transformed to a monoclinic one and the volume decreased by 4.5%. The monoclinic structure can be reproduced by defining an orthorhombic unit cell with $a=3.05$ Å, $b=3.28$ Å, and $c=4.40$ Å, which contains four atoms at positions $(-0.08,0,-0.08)$, $(0.08,0,0.42)$, $(0.42,0.5,0.08)$, and $(0.58,0.5,0.58)$. The x-ray pattern of this structure corresponds neither to the experimental pattern of Ca-IV nor to that of Ca-V, and therefore we proceeded to the following simulation.

Using the above structure with the orthorhombic unit cell and setting the GP parameters $W$ and $\delta h$ at 10 mRy and 20 mÅ, respectively, we started the main run and explored neighboring local minima on the GFE surface. In Fig. 1 we show the evolution of the angles and the length of the cell edges in the progress of the metasteps. Since the behavior of $\gamma$, $a$, and $b$ began to change around the 270th metastep, we switched the GP off by setting $W$ at 0 mRy and performed the relaxation run to confirm whether the system had escaped from the starting potential well. We found that the orthorhombic structure was transformed to a structure having another monoclinic lattice. The angle $\gamma$ increased from 90° to approximately 92° and $a$ and $b$ became equal. When we switched the GP off before reaching the 270th metastep, the structure returned to the starting orthorhombic structure. Here we note that bigger values of the parameters $W$ and $\delta h$ may accelerate the evolution speed, but skipping some local minima may happen for big values.

We found that the primitive unit cell of the monoclinic lattice has the dimensions of $a=3.16$ Å, $b/a=1.00$, $c/a=1.39$, and $\gamma=92.66°$ at 120 GPa and it consists of four atoms. The atomic positions are Ca(1)$=(-0.10,0.10,-0.06)$, Ca(2)$=(0.10,-0.10,0.44)$, Ca(1′)$=(0.40,0.60,0.06)$, and Ca(2′)$=(0.60,0.40,0.56)$. It can be viewed as a lattice consisting of two zigzag chains. The calcium atoms on each chain are shown by purple (dark gray) or blue (light gray) colors in Fig. 2. This structure can be redefined as an orthorhombic lattice by the choice of the double sized unit cell.

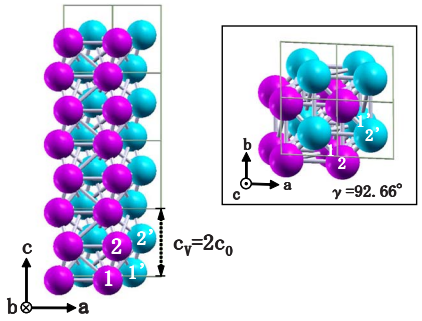


FIG. 2. (Color online) Structure of Ca-V obtained by an *ab initio* metadynamics simulation and its view along the $c$ axis (inset). The lattice consists of two zigzag chains along the $c$ axis, and calcium atoms on each chain are shown by purple (dark gray) or blue (light gray) colors, whose positions are numbered and written in the text. The length $c_0$ is the lattice constant $c$ for the lattice without the zigzag pattern.

We compare the x-ray diffraction patterns in Fig. 3, where the upper pattern is the experimental pattern[7] of Ca-V and the lower one is the zigzag structure. The comparison shows that the pattern of the zigzag structure matches the experimental pattern of Ca-V, including invisible shoulder peaks in the calculated pattern.

To find the difference in the x-ray patterns of Ca-IV and Ca-V, we compare the experimental x-ray patterns shown in Fig. 3 (upper figure) and Fig. 5 (upper figure). The most distinct change of the diffraction pattern is the appearance of a peak around $2\theta=17°$. If we analyze the peak using the

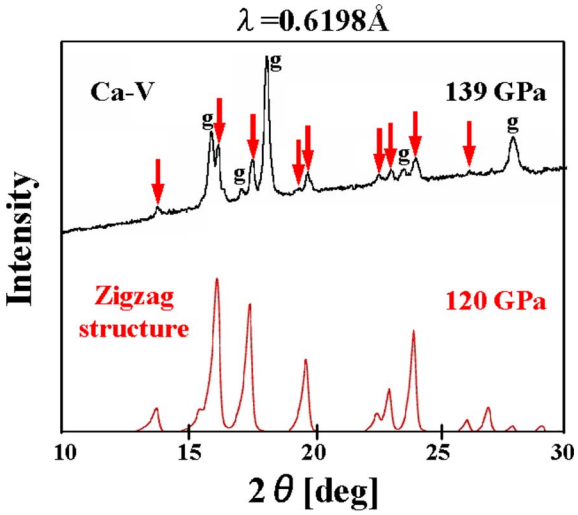


FIG. 3. (Color online) Comparison of the experimental x-ray diffraction pattern (Ref. 7) of Ca-V (upper figure) with that of the zigzag pattern which is obtained by *ab initio* metadynamics simulation (lower figure). In the upper figure, reflections from the Ca sample are indicated by arrows and those from a metal gasket by $g$.

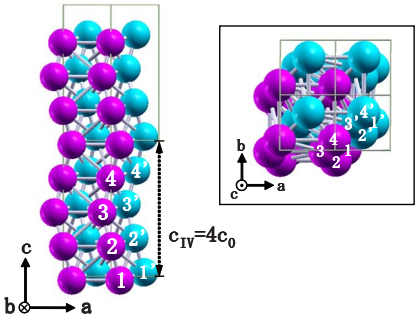


FIG. 4. (Color online) Structure of Ca-IV obtained by *ab initio* metadynamics simulation and its view along the $c$ axis (inset). The lattice consists of two helical chains along the $c$ axis, and calcium atoms on each chain are shown by purple (dark gray) or blue (light gray) colors, whose positions are numbered and written in the text. The length $c_0$ is the lattice constant $c$ for the structure without the helical modulation.

zigzag structure, the Miller indices of the peak around $2\theta = 17°$ are $(hkl)=(111)$. When we consider our zigzag pattern as a modulation along the $c$ axis in the primitive cell with no modulation, we get the modulation wave vector along the $c$ axis $q_c=0.5$. However, we have observed that the peak at $2\theta=17°$ in the calculated x-ray pattern disappears if we change the wave vector along the $c$ axis from $q_c=0.5$ to 0.25. Then we performed a MD simulation and structural optimization using an extended simulation cell of double size along the $c$ axis with modulation corresponding to $q_c=0.25$. The structure relaxed to another stable structure.

The structure obtained is the tetragonal lattice. The unit cell of the lattice has the dimensions $a=3.14$ Å, $b/a=1.00$, and $c/a=2.90$ at 120 GPa. If we denote the two helical chains by $A_o$ and $B_o$, the atoms on $A_o$ are aligned in the helical pattern consisting of four atoms along the $c$ axis: The atomic positions are Ca(1)=(0.18,0.01,−0.03), Ca(2)=(0.01,−0.18,0.22), Ca(3)=(−0.18,−0.01,0.47), and Ca(4)=(−0.01,0.18,0.72). The atoms on $B_o$ are aligned in a similar helical pattern, which is obtained by slightly rotating the four atoms on $A_o$ clockwise around the $c$ axis: The atomic positions are Ca(1′)=(0.68,0.49,0.03), Ca(2′)=(0.49,0.32,0.28), Ca(3′)=(0.32,0.51,0.53), and Ca(4′)=(0.51,0.68,0.78). This lattice can be viewed as one consisting of two helical chains (Fig. 4). We observe in Fig. 5 that the x-ray pattern of the helical structure matches that of Ca-IV.[7]

We compared the total energy of the helical structure of the two chains $A_o$ and $B_o$ with that of the two identical $A_o$ chains to see how much effect a slight rotation of the atomic positions has on the energy. As a result, the former is lower by 0.9 mRy/atom than the latter. This means that, although the difference between the helical patterns of the two chains $A_o$ and $B_o$ is slight, the rotation really lowers the energy of the helical structure.

In Fig. 6 we show the enthalpy differences among the sc (Ca-III), the helical, and the zigzag structures as functions of the pressure from 80 to 120 GPa. If the enthalpy curves are extrapolated to the low-pressure region, the enthalpy curve of the helical structure crosses that of the sc structure at

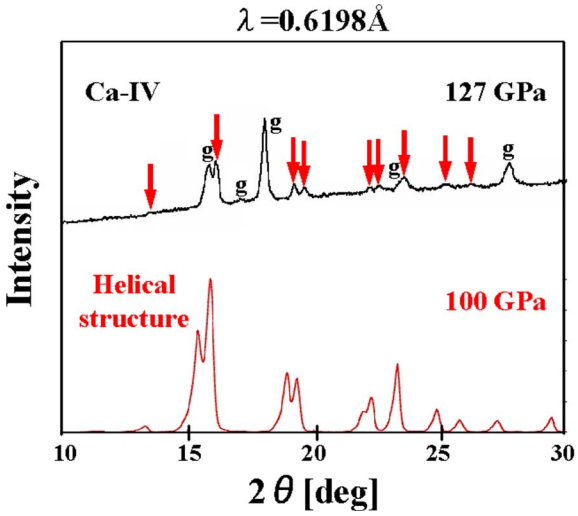


FIG. 5. (Color online) Comparison of the experimental x-ray diffraction pattern (Ref. 7) of Ca-IV (upper figure) with that of the helical structure which is obtained by *ab initio* MD simulation (lower figure). In the upper figure, reflections from the Ca sample are indicated by arrows and those from a metal gasket by $g$.

around 70 GPa. The enthalpy of the helical structure remains lowest up to 107 GPa, above which the enthalpy of the zigzag structure becomes lowest. The above estimated transition pressures are lower by about 30 GPa than the experimental transition pressures. The origin of this discrepancy between the transition pressures is not totally clear, but we have checked convergence of the total energy, changing the energy cutoff of the plane-wave basis and the number of mesh points used in the **k**-space integration. We checked also the equation of state (EOS) in the sc phase using the WIEN2K package which employs all-electron calculations in the GGA, and observed no significant change of the EOS between the two methods. Both methods gave a pressure that is

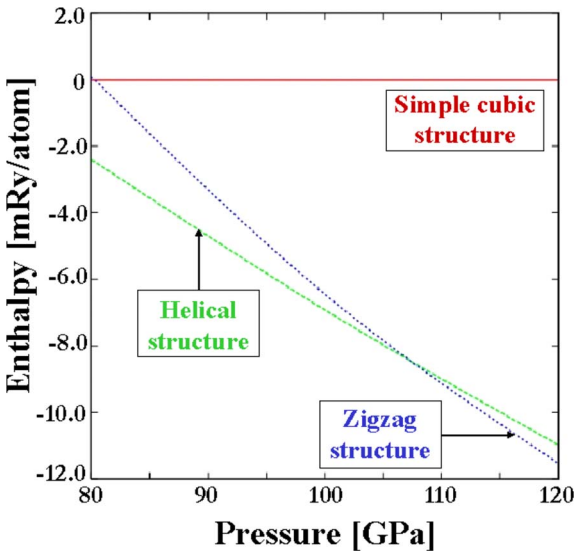


FIG. 6. (Color online) Comparison of the enthalpy curves between the simple cubic (Ca-III), the helical (the candidate for Ca-IV), and the zigzag (the candidate for Ca-V) structures.

in good agreement with experiment (32 GPa) at the volume $132a_0^3$/atom, but is lower by about 15 GPa than the experimental value, 113 GPa, at the volume $88a_0^3$/atom. We guess that the discrepancies in the EOS may come from inaccuracy in the GGA energy functional.

Finally we mention the periodicity of the modulation. The space group of Ca-IV is identified to be $P4_3$ ($C_4^4$) with atoms occupying two kinds of 4*a* sites. For the optimized structure given in this paper, the parameters for the atomic positions 4*a* are $(x_1,y_1,z_1)=(d_1,d_2,e_1)$ and $(x_2,y_2,z_2)=(1/2+d_1,1/2-d_2,-e_1)$ with $d_1=0.18$, $d_2=0.01$, and $e_1=-0.03$. The space group of Ca-V is *Cmca* ($D_{2h}^{18}$), which is orthorhombic, with atoms occupying 8*f* sites. The 8*f* site parameters can be defined as $(y,z)=(1/4+d_1,-1/4+e1)$ with $d_1=-0.10$ and $e_1=0.06$, after shifting the origin. The possibility remains, however, that Ca-IV or Ca-V has an incommensurately modulated structure, since in our theoretical calculations we have to impose periodic boundary conditions on the system. The experimental data for the pressure dependence of the side peaks will be helpful to determine the commensurability.

In this study, we found two candidate structures for Ca-IV and Ca-V by *ab initio* metadynamics and MD simulations. The candidate for Ca-IV is a tetragonal lattice with a helical atomic alignment. The appearance of the helical distortion under high pressure is a property that has been observed in another group-2 element, namely, Sr.[16] The candidate for Ca-V is an orthorhombic lattice with a zigzag atomic alignment. The good agreement of the x-ray diffraction patterns with the experiments shows that the structures of Ca-IV and Ca-V are very close to those predicted in this study. The only remaining exception is a possible incommensurate modulation with a $q$ vector close to the present value. Once the structures of Ca-IV and Ca-V are known, it will accelerate the theoretical investigation of the origin of the high $T_c$ in calcium.

The authors thank Y. Nakamoto and K. Shimizu for valuable discussion on the x-ray powder patterns. Computations were performed at the Institute for Molecular Science, Okazaki, Aichi, Japan, and at ISSP, University of Tokyo. This work was partially supported by Grants-in-Aid for Scientific Research in Priority Area (No. 17064013 and No. 19051016) of the Ministry of Education, Culture, Sports, Science, and Technology, Japan. It was also supported by Research Fellowships for Young Scientists (No. 19.1723), a Grant-in-Aid for Scientific Research (No. 15GS0213), and the 21st COE Program of the Japan Society for the Promotion of Science (JSPS).

*ishikawa@aquarius.mp.es.osaka-u.ac.jp

[1] M. I. McMahon and R. J. Nelmes, Chem. Soc. Rev. **35**, 943 (2006).
[2] T. Kikegwa and H. Iwasaki, Acta Crystallogr., Sect. B: Struct. Sci. **39**, 158 (1983).
[3] Y. Akahama, M. Kobayashi, and H. Kawamura, Phys. Rev. B **59**, 8520 (1999).
[4] T. Ishikawa, H. Nagara, K. Kusakabe, and N. Suzuki, Phys. Rev. Lett. **96**, 095502 (2006).
[5] H. Fujihisa, Y. Akahama, H. Kawamura, Y. Ohishi, Y. Gotoh, H. Yamawaki, M. Sakashita, S. Takeya, and K. Honda, Phys. Rev. Lett. **98**, 175501 (2007).
[6] H. Olijnyk and W. B. Holzapfel, Phys. Lett. **100A**, 191 (1984).
[7] T. Yabuuchi, Y. Nakamoto, K. Shimizu, and T. Kikegawa, J. Phys. Soc. Jpn. **74**, 2391 (2005).
[8] T. Yabuuchi, T. Matsuoka, Y. Nakamoto, and K. Shimizu, J. Phys. Soc. Jpn. **75**, 83703 (2006).
[9] K. J. Dunn and F. P. Bundy, Phys. Rev. B **25**, 194 (1982).
[10] H. L. Skriver, Phys. Rev. Lett. **49**, 1768 (1982).
[11] R. Ahuja, O. Eriksson, J. M. Wills, and B. Johansson, Phys. Rev. Lett. **75**, 3473 (1995).
[12] R. Martoňák, A. Laio, and M. Parrinello, Phys. Rev. Lett. **90**, 075503 (2003).
[13] S. Baroni, A. D. Corso, S. de Gironcoli, and P. Giannozzi, computer code PWSCF (http://www.pwscf.org/).
[14] J. P. Perdew, in *Electronic Structure of Solids '91*, edited by P. Ziesche and H. Eschrig (Akademie-Verlag, Berlin, 1991), p. 11.
[15] P. Blaha, K. Schwarz, G. K. H. Madsen, D. Kvasnicka, and J. Luitz, computer code WIEN2K (Karlheinz Schwarz, Technische Wien, Austria, 2001).
[16] T. Bovornratanaraks, D. R. Allan, S. A. Belmonte, M. I. McMahon, and R. J. Nelmes, Phys. Rev. B **73**, 144112 (2006).